Photo-double-ionization of He-like and Be-like systems in excited states within an intermediate-energy *R*-matrix framework

M. W. McIntyre and M. P. Scott
School of Mathematics and Physics, Queen's University Belfast, Belfast, BT7 1NN, United Kingdom
(Received 22 January 2014; published 17 April 2014)

In this article we apply the intermediate-energy *R*-matrix method to photo-double-ionization of the metastable $1s2s\ ^{1,3}S^e$ and $1s2p\ ^{1,3}P^o$ states of He, O^{6+}, and Ne^{8+}, along with the $1s^2\ 2s2p\ ^{1,3}P^o$ and $1s^2\ 2s3s\ ^{1,3}S^e$ states of Be, O^{4+}, and Ne^{6+}. We compare our results with other theoretical data where possible and achieve excellent agreement. We examine trends between the various excited states and ground states of the systems.

DOI: 10.1103/PhysRevA.89.043418 PACS number(s): 32.80.Fb

I. INTRODUCTION

In this paper we apply the intermediate energy *R*-matrix (IERM) method of Scott *et al*. [1] to photo-double-ionization of the metastable $1s2s\ ^{1,3}S^e$ and $1s2p\ ^{1,3}P^o$ states of He, O^{6+}, and Ne^{8+}, along with the $1s^2\ 2s2p\ ^{1,3}P^o$ and $1s^2\ 2s3s\ ^{1,3}S^e$ states of Be, O^{4+}, and Ne^{6+}. This method proved very successful when applied to photo-double-ionization from the ground states of He-like and Be-like atoms and ions, as demonstrated by McIntyre *et al*. [2].

Photo-double-ionization is an interesting study of electron-electron interactions, since only one electron absorbs the photon and then transfers some amount of energy to the second electron in order to ionize it, mostly through electron-electron repulsion. Photo-double-ionization of the He isoelectronic sequence is also of interest for astrophysical purposes. For example, McLaughlin [3] reports that C^{3+}, N^{4+}, O^{6+}, and Ne^{8+} are all abundant in the warm-hot intergalactic medium and of importance in determining the mass of missing baryons [4,5].

As far as we are aware, experimental measurements of photo-double-ionization cross sections for these ions have been limited to photo-double-ionization from the ground states, see, e.g., Refs. [6,7]. Theoretical efforts to calculate the photo-double-ionization from excited states of He-like systems have so far concentrated on the metastable $1s2s\ ^{1,3}S^e$ states, and a wide variety of techniques have been employed. Van der Hart and Feng [8] used a *B*-spline-based *R*-matrix technique to calculate the ratio of double to total ionization in the photoionization of He, Li^+, Be^{2+}, C^{3+}, and O^{6+} in the $1s2s\ ^{1,3}S^e$ excited states. Photo-double-ionization from the excited $1s2s\ ^{1,3}S^e$ states of Li^+ were examined by McLaughlin [3] using the *R*-matrix with pseudostates (RMPS) method and Kleiman *et al*. [9], who used the time-dependent close-coupling (TDCC) method. Colgan and Pindzola [10] studied photo-double-ionization from the excited $1s2s\ ^{1,3}S^e$ states of He using the TDCC method.

For Be, theoretical efforts to calculate the photo-double-ionization cross section are focused on the $1s^2\ 2s2p\ ^{1,3}P^o$ states. Griffin *et al*. [11] used the RMPS method to calculate photo-double-ionization cross sections from these states and Yip *et al*. [12] studied photo-double-ionization of Be in the $1s^2\ 2s2p\ ^3P^o$ excited state and Li in the $1s^2 2p\ ^2P^o$ state using a method based on the finite-element discrete-variable representation and exterior complex scaling.

The remainder of this paper is organized as follows: In Sec. II we present a summary of the theory and description of the computational models used in the calculations. We then present and discuss our results in Sec. III. Finally, we draw conclusions in Sec IV.

II. COMPUTATIONAL MODELS

The IERM theory of photoionization is an extension of the *R*-matrix theory of photoionization of Burke and Taylor [13] and the theory has been well documented in publications by Scott *et al*. [1] and McIntyre *et al*. [2]; we will therefore provide only basic details that are relevant to the discussion here. In the dipole length approximation, the total cross section for photoionization by unpolarized light is given by

$$\sigma = \frac{8\pi^2\alpha a_o^2\omega}{3(2L_i+1)}\sum_{l_f L}|\langle\Psi_f^-||M||\Psi_i\rangle|^2, \qquad (1)$$

where α is the fine structure constant, a_0 is the Bohr radius of hydrogen, ω is the energy of the incident photon in atomic units, and $\langle\Psi_f^-||M||\Psi_i\rangle$ are reduced dipole matrix elements. The initial bound state, Ψ_i, is defined by the quantum numbers $L_i S_i \Pi_i$, while the final "ion + electron" continuum state, Ψ_f^-, has quantum numbers $LS\Pi$. The final state of the residual ion is defined by $L_f S_f \Pi_f$. Configuration space is divided by a sphere of radius a centered on the target nucleus and, outside the sphere, electron exchange and correlation are neglected. Inside the sphere, both Ψ_i and Ψ_f^- are expanded in terms of appropriate energy-independent *R*-matrix basis states which are themselves expanded as

$$\Theta_k^p(\mathbf{r}_1,\mathbf{r}_2) = \sum_{n_1 l_1 n_2 l_2}\chi^p_{n_1 l_1 n_2 l_2}(\mathbf{r}_1,\mathbf{r}_2)\beta^p_{n_1 l_1 n_2 l_2}, \qquad (2)$$

where p corresponds to the quantum numbers of the initial or final state. The two-electron functions χ are products of one-electron radial functions and angular functions. The radial functions consist of the physical orbitals of the residual one-electron or quasi-one-electron ion and a number of nonphysical pseudo-orbitals. The pseudo-orbitals give rise to nonphysical pseudostates, a certain number of which lie above the ionization threshold of the residual ion. Summing the cross sections to these positive energy pseudostates allows us to evaluate the photo-double-ionization cross section. An extended set of these radial functions (labeled "continuum functions" in this case) are used to represent the "bound"

photoelectron in the initial state and the ejected photoelectron in the final state. The coefficients β are obtained by diagonalizing a two-electron Hamiltonian matrix for either the initial or final state. We ensure that the R-matrix radius is chosen large enough to completely envelope the initial state so there is no contribution to the reduced dipole matrix elements from the external region. In order to slightly improve the calculated energy we add a small correction to the appropriate element of the Hamiltonian matrix of the initial state prior to diagonalization.

A. He-like

In this section we present details for the calculation of photo-double-ionization cross sections of He, O^{6+}, and Ne^{8+} in $1s2s\ ^{1,3}S^e$ and $1s2p\ ^{1,3}P^o$ excited states. Dipole selection rules allow only $^{1,3}P^o$ final states for the $1s2s\ ^{1,3}S^e$ initial states. For the $1s2s\ ^{1,3}P^o$ initial states however, there are three possible final states for each spin: $^{1,3}S^e$, $^{1,3}P^e$, and $^{1,3}D^e$. Spin is conserved in each case and the cross sections for each final state are summed to give the total cross section. For each ion, physical orbitals $1s,2s,2p,3s,3p,3d,4s,4p,4d,4f$ of the relevant H-like ion are included and augmented by pseudo-orbitals $n = 5,\ldots,38$ and angular momentum $l = 0,\ldots,5$. It is worth noting that the He-like ground-state calculations presented in Refs. [1,2] had fully converged by $l = 3$. As mentioned by van der Hart and Feng [8] and Colgan and Pindzola [10], the additional angular momenta are required due to the more diffuse nature of the exited states compared to the ground states. Seventy continuum functions were included for each angular momentum. As stated in Scott *et al.* [1], it is important to have a very dense pseudostate basis in the energy region just above the double ionization threshold where the cross section is varying rapidly. This region is also particularly sensitive to electron correlation, and for both these reasons we select a relatively large R-matrix boundary radius to evaluate the photo-double-ionization cross section in this region. We then select a smaller radius to evaluate the photo-double-ionization cross section at higher energies so the same number of pseudo-states span a larger energy region: Details of the two radii used for each atom or ion are presented in Table I. Of the total 213 H-like target states, there are at least 167 that have positive energy for the smaller radius calculation and at least 161 for the larger radius calculation. We apply a small correction to the appropriate element of the two-electron Hamiltonian matrix prior to diagonalization in order to bring the calculated energy of the initial state into agreement with values from the NIST [14] atomic spectra database: The correction and energies are detailed in Table II.

TABLE I. R-matrix radii in atomic units selected for low and high energy calculations for each He-like atom or ion.

Atom or ion	Low energy radius	High energy radius
He	70	40
O^{6+}	20	10
Ne^{8+}	16	8

TABLE II. Calculated bound-state energies in atomic units for each He-like atom or ion along with the correction added to the Hamiltonian matrix prior to diagonalization to improve agreement with values from NIST.

Atom or ion	State	Calculated	Correction	NIST[a]
He	^1S	−2.1456	0.000	−2.145
	^3S	−2.1752	0.000	−2.1750
	^1P	−2.1238	0.000	−2.1236
	^3P	−2.1331	0.000	−2.1330
O^{6+}	^1S	−38.2533	−0.0339	−38.2873
	^3S	−38.5444	−0.0333	−38.5777
	^1P	−38.0722	−0.0290	−38.1013
	^3P	−38.2687	−0.02942	−38.2982
Ne^{8+}	^1S	−60.2895	−0.0776	−60.3670
	^3S	−60.6683	−0.0756	−60.7440
	^1P	−60.0528	−0.0685	−60.1216
	^3P	−60.3168	−0.0655	−60.3823

[a]NIST [14].

B. Be-like

We now describe the calculation of the photo-double-ionization cross section of Be, O^{4+}, and Ne^{6+} from the $1s^2\ 2s2p\ ^{1,3}P^o$ and $1s^2\ 2s3s\ ^{1,3}S^e$ excited states. Again, photo-double-ionization from the $1s^2\ 2s2p\ ^{1,3}P^o$ initial states have three possible final states and the $1s^2\ 2s3s\ ^{1,3}S^e$ states only one. The calculations here are again split into two energy regions, with a larger radius being selected for the region just above the threshold: These radii are presented in Table III. The physical orbitals $2s$, $2p$, $3s$, $3p$, $3d$, $4s$, $4p$, $4d$, and $4f$ of the relevant Li-like ion are included, where a core potential (detailed in Ref. [2]) has been used to represent the "frozen" $1s^2$ core. For the smaller radius calculation, physical orbitals are augmented by pseudo-orbitals $n = 5,\ldots,35$ and orbital angular momentum $l = 0,\ldots,6$. Similarly to the He-like calculations, it is also worth noting here that calculation of the photo-double-ionization cross section for Be-like ions in the ground state [2] had fully converged by $l = 5$. This gives a total of 233 target states, of which at least 176 are above the double ionization threshold. Fifty continuum functions were included per angular momentum. In order to keep the size of the calculation tractable, for the larger radius calculation we included fewer pseudo-orbitals and continuum functions. Pseudo-orbitals with $n = 5,\ldots,32$ and 45 continuum functions per angular momentum were found to span the desired energy range. The same orbital angular momentum of $l = 0,\ldots,6$ were included in the larger radius calculations. The calculated single ionization potential for each state prior to the correction being made to the Hamiltonian matrix are detailed in Table IV.

TABLE III. R-matrix radii in atomic units selected for low and high energy calculations for each Be-like atom or ion.

Atom or ion	Low energy radius	High energy radius
Be	63.18	39.88
O^{4+}	22.98	15.11
Ne^{6+}	17.25	11.89

TABLE IV. Calculated bound-state ionization potentials in atomic units for each Be-like atom or ion compared with values from NIST.

Atom or ion	State	Calculated	NIST[a]
Be	^1P	0.1514	0.1487
	^3P	0.2464	0.2425
	^1S	0.0941	0.0935
	^3S	0.1069	0.1054
O^{4+}	^1P	3.4683	3.4621
	^3P	3.8210	3.8111
	^1S	1.6338	1.6283
	^3S	1.7018	1.6935
Ne^{6+}	^1P	6.6228	6.6376
	^3P	7.0988	7.1057
	^1S	3.0634	3.0689
	^3S	3.1576	3.1595

[a]NIST [14].

III. RESULTS

A. He-like

In Fig. 1 we compare our results for the photo-double-ionization cross section of He in the $1s2s\ ^{1,3}S^e$ excited states with other theoretical data. We achieve excellent agreement with both the CCC data of Kheifets *et al*. [15] and the TDCC data of Colgan and Pindzola [10] across the range of energies apart from the height of the peak at 70 eV, where our results lie slightly lower than the CCC results for both initial states. We also include a fit to the shape function of Pattard [16] to the current data in Fig. 1. Pattard showed that the cross section for multiple photoionization processes in which all electrons are ionized can be parameterized as follows:

$$\sigma(\epsilon) = \sigma_M x^\alpha \left(\frac{\alpha + 7/2}{\alpha x + 7/2}\right)^{(\alpha+7/2)}, \tag{3}$$

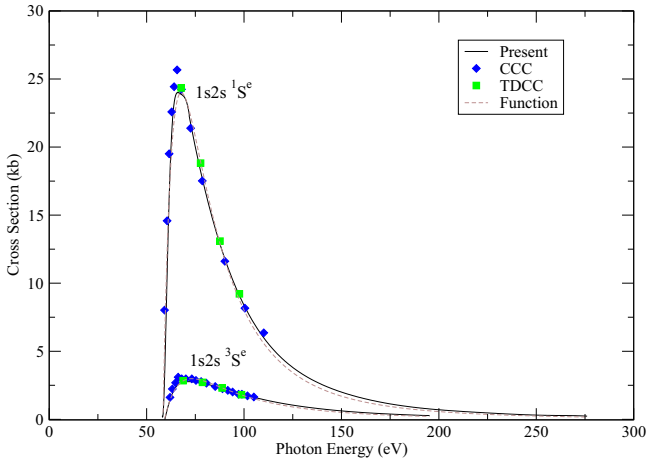

FIG. 1. (Color online) Photo-double-ionization cross section for the $1s2s\ ^{1,3}S^e$ states of He. Black solid line: Present calculation; blue diamonds: CCC data Kheifets *et al*. [15]; green squares: TDCC data of Colgan and Pindzola [10]; brown dashed line: shape function of Pattard [16] [Eq. (3)] fit to the current data.

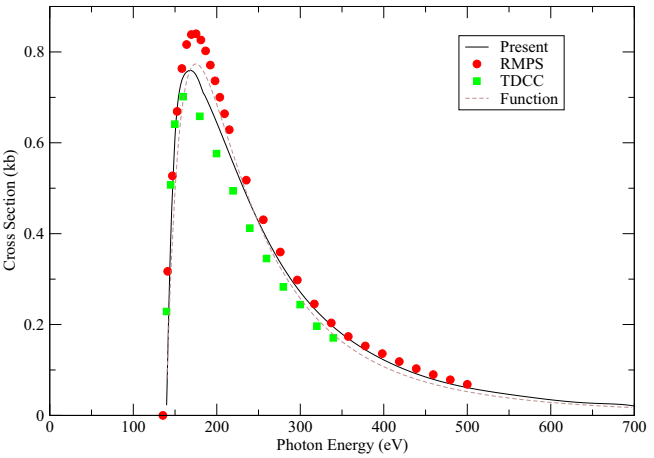

FIG. 2. (Color online) Photo-double-ionization cross section for the $1s2s\ ^3S^e$ state of Li^+. Black solid line: Present calculation; red circles: RMPS data of McLaughlin [3]; green squares: TDCC data of Kleiman [9]; brown dashed line: shape function of Pattard [16] [Eq. (3)] fit to the current data.

where σ_M is the maximum value of the cross section and the Wannier threshold exponent [17], α, depends on the charge of the residual ion, Z_r, and is given by

$$\alpha = \frac{1}{4}\left[\left(\frac{100Z_r - 9}{4Z_r - 1}\right)^{1/2} - 1\right]; \tag{4}$$

$x = \epsilon/\epsilon_M$, where ϵ is the excess energy above the double-ionization threshold and ϵ_M is the energy value of the maximum in the photo-double-ionization cross section. Several authors have shown that the shape function can successfully parametrize the cross section for multiple ionization by photon impact even in cases were all electrons are not ionized (see, e.g., Refs. [2,18]). When fitting the shape function to the current data, σ_M and ϵ_M were set as adjustable parameters. There is only slight deviation of the current data from the shape function. A fit of the shape function is also included in Fig. 2 where we compare our results of the photo-double-ionization of Li^+ with the recent RMPS calculation of McLaughlin [3] and the TDCC calculation of Kleiman [9]. We show excellent agreement with both calculations for incident photon energies beneath 154 eV (just before the peak in Fig. 2), after which our data lie slightly above the TDCC data and slightly below the RMPS data. The present data are shown to deviate from the shape function of Pattard [16] slightly more for the photo-double-ionization cross section for Li^+ in the $1s2s\ ^3S^e$ excited state than for He in the same initial state. However, the shape function still provides a reasonable parameterization of the current data.

In Fig. 3, the photo-double-ionization cross sections for the $1s2s\ ^{1,3}S^e$ and $1s2p\ ^{1,3}P^o$ excited states of He, O^{6+}, and Ne^{8+} are presented along with the photo-double-ionization cross section for the $1s^2\ ^1S^e$ ground-state data from McIntyre *et al*. [2]. One of the most obvious features in Fig. 3 is that the magnitude of the photo-double-ionization cross section of the ground state relative to that of the excited states decreases as Z increases. For the He data we see that at photon energies above 100 eV, photo-double-ionization of the ground state is more

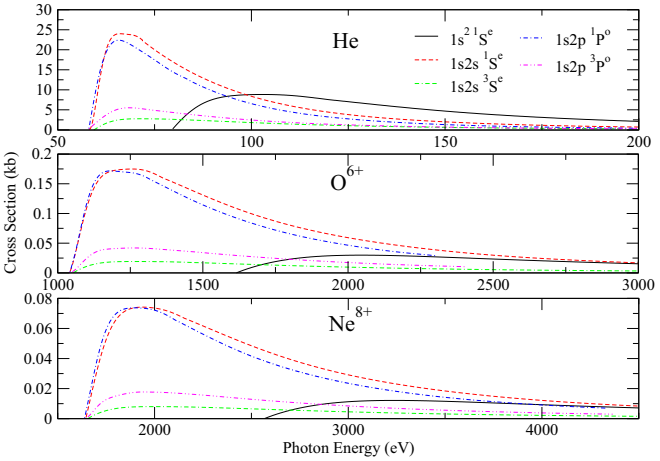

FIG. 3. (Color online) Photo-double-ionization cross section for the ground and excited S and P states of He, O^{6+}, and Ne^{8+}.

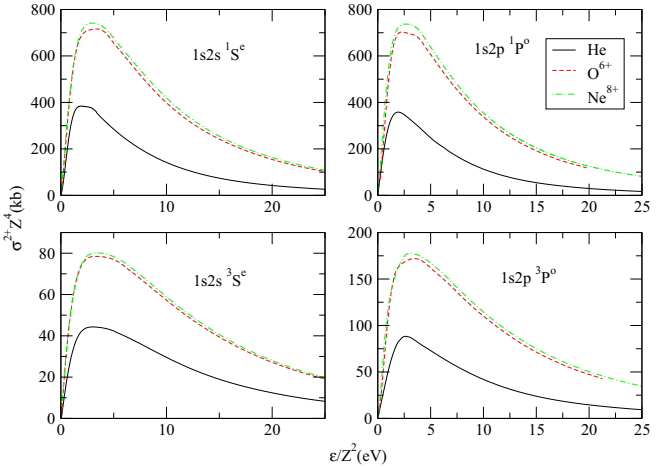

FIG. 4. (Color online) Photo-double-ionization cross section from the ground, and S and P excited states of He, O^{6+}, and Ne^{8+} multiplied by Z^4 and plotted against the excess energy above the double ionization threshold divided by Z^2.

likely than any of the excited states. However for O^{6+} and Ne^{8+} we see that photo-double-ionization of the $1s2s\ {}^1S^e$ state is the most dominant at all energies; this was also observed by van der Hart and Feng [8]. A feasible explanation for this is simply that photo-double-ionization of the ground state is comparatively less likely than it is for the excited singlet states since the ground state is increasingly strongly bound compared to the excited states as we examine systems with increasing Z. In fact the percentage difference in binding energy between the $1s2s\ {}^1S^e$ and the $1s^2\ {}^1S^e$ initial states is roughly proportional to the percentage decrease in the maximum of the photo-double-ionization cross section. The same behavior is also observed between the $1s2p\ {}^1P^o$ initial state and the ground state. We see that the photo-double-ionization cross section of the $1s2p\ {}^1P^o$ initial state is greater than that of the ground state at higher energies, relative to the double-ionization threshold of the ground state, for O^{6+} and Ne^{8+}; note that in Fig. 3 the curve for the $1s2p\ {}^1P^o$ initial state of He intersects the curve for the ground state just before its peak, while for O^{6+} and Ne^{8+} the two curves intersect well after the peak in the ground-state curve. In all cases the photo-double-ionization cross section for the triplet excited states is smaller than it is for singlet states of the same L: This was also observed in other studies (see, e.g., Refs. [8,9,19]). This occurs because the spin part of the wave function is symmetric in the triplet state, and therefore the spatial part must be antisymmetric. The electrons are therefore much less likely to be close together and an interaction between the two that is strong enough to ionize the second electron is also less likely. In Fig. 3 we see that the the photo-double-ionization cross section for the $1s2s\ {}^1S$ initial state of He is very slightly larger that that of the $1s2p\ {}^1P$ initial state. The same is true for O^{6+} and Ne^{8+}. Considering the photo-double-ionization of the triplet states, however, we note that for all the ions the cross section from the $1s2p\ {}^3P^o$ state is larger than the cross section from the $1s2s\ {}^3S^e$ state.

For each of the ${}^{1,3}P^o$ initial states the total cross section consists of a sum of S^e, P^e, and D^e final states. For the singlet initial state, the D^e final state contributes the most followed by the S^e state, while the P^e final state contributes very weakly. For the triplet initial state the contribution from the S^e and D^e final states is considerably less than those from the singlet; however, the P^e contribution actually increases between the singlet and triplet cases and gives the largest contribution of the three final states.

It is interesting to examine if the simple Z scaling of the photo-double-ionization cross sections for the He-like systems in their ground states proposed by Kornberg and Miraglia [20] is applicable to photo-double-ionization cross sections from the various excited states. In Fig. 4 we show the photo-double-ionization cross section for He, O^{6+}, and Ne^{8+} in various excited states multiplied by Z^4 and plotted against the excess energy above the double ionization threshold, ϵ, divided by Z^2. The scaling law of Kornberg and Miraglia [20] was derived from a scaled Schrödinger equation where the Z dependence of the r_{12}^{-2} term is neglected; this results in the scaling only being exact as Z approaches infinity. This means that even

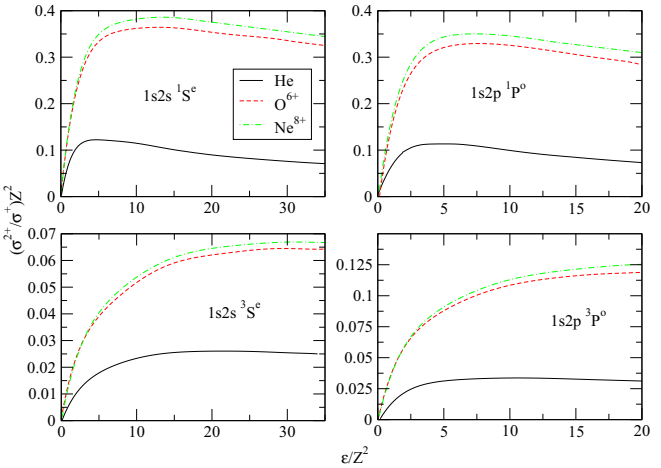

FIG. 5. (Color online) Ratio of double to single photoionization from the ground and S and P excited states of He, O^{6+}, and Ne^{8+} multiplied by Z^2 and plotted against the excess energy above the double ionization threshold divided by Z^2.

for the ground states the scaled photo-double-ionization cross sections for low-Z ions slightly deviate from the curve shared by ions with large Z. While data for more ions would be useful in analyzing the scaling in the current case, the scaled cross sections in Fig. 4 do appear to be converging on a common curve as Z increases. Van der Hart and Feng [8] examined the scaling of the ratio of double ionization to total ionization for various He-like species in $1s2s\ ^1S$ excited states and found no simple Z scaling law that applied for systems up to $Z = 6$. However, in Fig. 5 we present scaled ratio data which appear to be converging as Z increases.

B. Be-like

In Fig. 6 we compare our results for the photo-double-ionization cross section of Be in the $1s^2 2s2p\ ^3P^o$ excited state with data from the RMPS calculation of Griffin *et al*. [11] and data from a hybrid atomic orbital with numerical grid method based on the finite-element discrete-variable representation and exterior complex scaling by Yip *et al*. [12]. Agreement is excellent in both cases. We note that Yip *et al*. [12] commented that the height of the maximum in their photo-double-ionization cross section from the $1s^2 2s2p\ ^1P^o$ excited state was 15.6 kb, and in our present calculation the maximum is 5.7% higher at 17.5 kb. We also include a fit of the shape function of Pattard [16] to the data presented in Fig. 6 and again see only slight differences between the two. This is interesting as it shows that the shape function, which was originally developed to parametrize the cross section for multiple photoionization processes in which all electrons are ionized, gives a good means of parameterizing the photo-double-ionization cross section from excited states in cases where there is not total break up of the target.

In Fig. 7 the photo-double-ionization cross section from the $1s^2\ 2s2p\ ^{1,3}P^o$ and $1s^2\ 2s3s\ ^{1,3}S^e$ excited states of Be, O^{4+}, and Ne^{6+} are plotted together with the respective ground-state

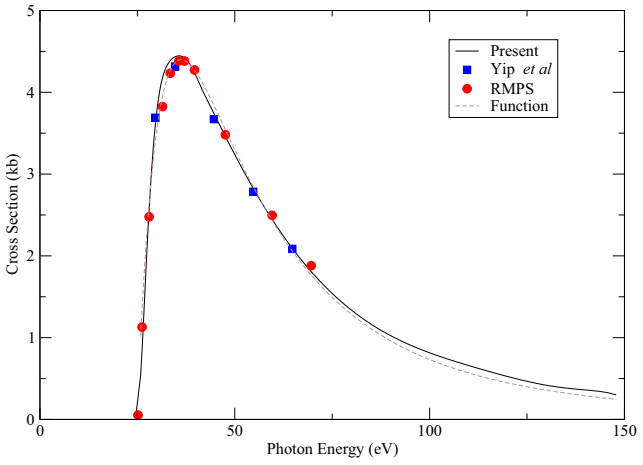

FIG. 6. (Color online) Photo-double-ionization cross section for the $1s^2 2s2p\ ^3P$ state of Be. Black solid line: Present calculation; red circles: RMPS data of Griffin *et al* [11]; blue squares: data from a hybrid atomic orbital with numerical grid method based on the finite-element discrete-variable representation and exterior complex scaling by Yip *et al*. [12]; brown dashed line: shape function of Pattard [16] [Eq. (3)] fit to the current data.

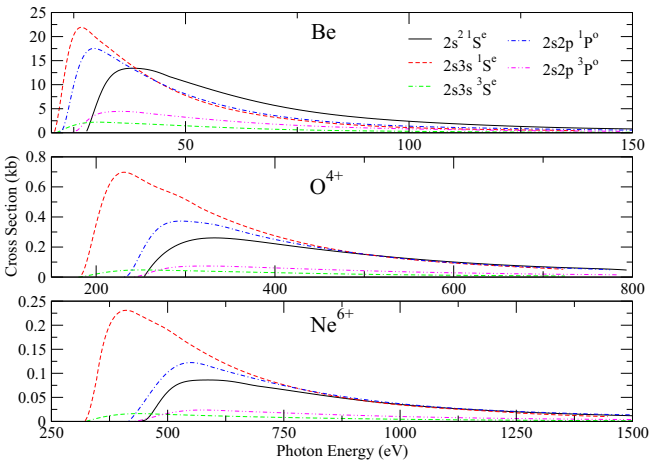

FIG. 7. (Color online) Photo-double-ionization cross section from the ground and S and P excited states of Be, O^{4+}, and Ne^{6+}.

results from McIntyre *et al*. [2]. For Be, the photo-double-ionization cross section for the ground state is larger than all of the excited states above a photon energy of 39 eV, which is close to the peak in the ground-state curve. For O^{4+}, however, the ground-state curve intercepts the other singlet curves well after the peak in the ground-state curve, at around 507 eV. The photo-double-ionization cross section for the ground state of Ne^{6+} is larger than that of the $1s^2\ 2s3s\ ^{1,3}S^e$ excited state above 922 eV, which is again well above the peak in the ground-state curve. The photo-double-ionization cross section for the $1s^2\ 2s2p\ ^1P^o$ excited state remains larger than the ground state for all photon energies examined in the the current study. The percentage difference between the photon energy required for double ionization of the ground and $1s^2 2s2p\ ^1P^o$ excited states, and between the ground and $1s^2\ 2s3s\ ^1S^e$, increases with Z. The percentage difference in the maximum of the photo-double-ionization cross section also increases with Z; however, the percentage differences are not quite proportional.

For the $1s^2\ 2s2p\ ^{1,3}P^o$ excited states of each system studied, the photo-double-ionization cross section to the S^e and D^e final states are larger for the singlet than for the triplet, and similarly to the He-like calculations, the photo-double-ionization cross section to the P^e final state for each target is larger for the triplet, again giving the largest contribution to the total for the triplet states. Yip *et al*. [12] also reported this feature in their singly differential cross sections of the same excited states of Be.

Many authors have observed that photo-double-ionisation cross sections may be scaled using the energy of the second ionization potential or an effective nuclear charge derived from it. For example, Mikhailov *et al*. [21,22] and Hoszowska *et al*. [23,24] applied this principle to photo-double-ionization of the K shell of neutral atoms and Wehlitz *et al*. [25] and Bluett *et al*. [26] applied it to scaling the energy in the ratio of double to single photoionzation of neutral atoms. It is interesting to examine how the photo-double-ionization cross sections for Be-like atoms and ions in the various excited states studied in this paper scale according to these principles since the screening effect of the $1s$ electrons should be accounted for. In Fig. 8 we show the photo-double-ionization cross section

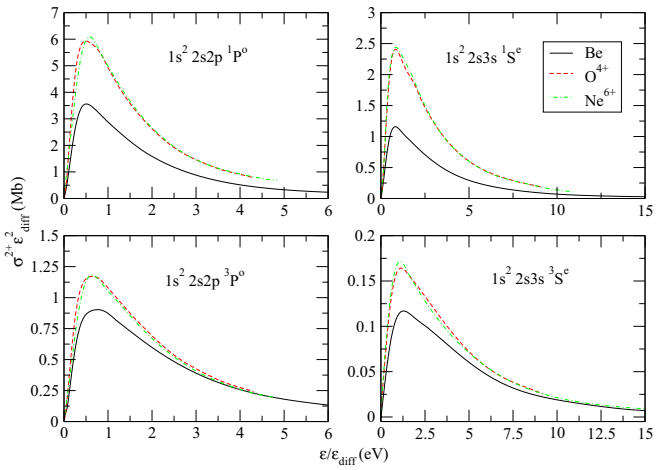

FIG. 8. (Color online) Photo-double-ionization cross section from the ground and S and P excited states of Be, O^{4+}, and Ne^{6+} multiplied by $\epsilon_{\rm diff}^2$ and plotted against the excess energy above the double ionization threshold divided by $\epsilon_{\rm diff}$.

of Be, O^{4+}, and Ne^{6+} in various excited states multiplied by $\epsilon_{\rm diff}^2$ and plotted against the excess energy above the double ionization threshold divided by $\epsilon_{\rm diff}$, where $\epsilon_{\rm diff}$ difference between the double, E_2, and single, E_1, ionization thresholds,

$$\epsilon_{\rm diff} = E_2 - E_1. \tag{5}$$

We see in Fig. 8 that when the photo-double-ionisation cross sections of Be-like atoms in excited initial states are scaled in the manner previously described they follow a similar trend to the scaled photo-double-ionisation cross sections of He-like atoms presented in Fig. 4. In the case of He-like atoms an effective nuclear charge derived from $\epsilon_{\rm diff}$ would simply be the nuclear charge, thus the present scaling is equivalent to the Z^2 scaling law of Kornberg and Miraglia [20] shown in Figs. 4 and 5. In cases where the ionized electrons are in different shells the energy of the lower shell is used as the single ionization threshold in this scaling.

IV. CONCLUSIONS

We have used the IERM approach to photo-double-ionization of the metastable $1s2s\ ^{1,3}S^e$ and $1s2p\ ^{1,3}P^o$ states of He, O^{6+}, and Ne^{8+}, and the $1s2s\ ^3S^e$ state of Li^+, along with the $1s^2\ 2s2p\ ^{1,3}P^o$ and $1s^2\ 2s3s\ ^{1,3}S^e$ states of Be, O^{4+}, and Ne^{6+}. We compare our data for He with the CCC data of Kheifets *et al.* [15] and the TDCC data of Colgan and Pindzola [10], obtaining excellent agreement with both. For Li^+ we obtain good agreement with RMPS data of McLaughlin [3] and the TDCC data of Kleiman [9]. Finally, for Be, the agreement between our data and the RMPS data of Griffin *et al.* [11] and data from a method based on finite-element discrete-variable representation by Yip *et al.* [12] is excellent. The shape function of Pattard [16] was found to parametrize the photo-double-ionization cross section well for excited states of both He-like and Be-like atoms and ions. We then examined trends in the photo-double-ionization cross section between the various excited states and the ground states. Scaling relations [2,20] that have been previously applied to the photo-double-ionization cross section of He-like and Be-like atoms and ions with $Z \leqslant 10$ in the ground state were applied to He-like and Be-like atoms and ions in excited states and found to be less appropriate for the same systems in excited states.

ACKNOWLEDGMENTS

M.W.McI was supported by a Northern Ireland DEL postgraduate studentship.

[1] M. P. Scott, A. J. Kinnen, and M. W. McIntyre, Phys. Rev. A **86**, 032707 (2012).
[2] M. W. McIntyre, A. J. Kinnen, and M. P. Scott, Phys. Rev. A **88**, 053413 (2013).
[3] B. M. McLaughlin, J. Phys. B: At. Mol. Opt. Phys. **46**, 075204 (2013).
[4] F. Nicastro, M. Smita, M. Elvis, J. Drake, F. Taotao, F. Antonella, K. Yair, M. Hermann, W. Rik, and Z. Andreas, Nature **433**, 495 (2005).
[5] L. Zappacosta, F. Nicastro, Y. Krongold, and R. Maiolino, Astrophys. J. **753**, 137 (2012).
[6] R. Wehlitz, D. Lukic, and J. B. Bluett, Phys. Rev. A **71**, 012707 (2005).
[7] J. A. R. Samson, W. C. Stolte, Z.-X. He, J. N. Cutler, Y. Lu, and R. J. Bartlett, Phys. Rev. A **57**, 1906 (1998).
[8] H. W. van der Hart and L. Feng, J. Phys. B: At. Mol. Opt. Phys. **34**, L601 (2001).
[9] U. Kleiman, M. S. Pindzola, and F. Robicheaux, Phys. Rev. A **72**, 022707 (2005).
[10] J. Colgan and M. S. Pindzola, Phys. Rev. A **67**, 012711 (2003).
[11] D. C. Griffin, M. S. Pindzola, C. P. Ballance, and J. Colgan, Phys. Rev. A **79**, 023413 (2009).
[12] F. L. Yip, C. W. McCurdy, and T. N. Rescigno, Phys. Rev. A **81**, 063419 (2010).
[13] P. G. Burke and K. T. Taylor, J. Phys. B: At. Mol. Opt. Phys. **8**, 2620 (1975).
[14] A. Kramida, Yu. Ralchenko, J. Reader, and NIST ASD Team (2012). NIST Atomic Spectra Database (ver. 5.0), National Institute of Standards and Technology, Gaithersburg, MD, http://physics.nist.gov/asd.
[15] A. S. Kheifets, A. Ipatov, M. Arifin, and I. Bray, Phys. Rev. A **62**, 052724 (2000).
[16] T. Pattard, J. Phys B At. Mol. Opt. Phys. **35**, L207 (2002).
[17] G. H. Wannier, Phys. Rev. **90**, 817 (1953).
[18] R. Wehlitz, Adv. At. Mol. Opt. Phys. **58**, 1 (2010).
[19] R. C. Forrey, H. R. Sadeghpour, J. D. Baker, J. D. Morgan, and A. Dalgarno, Phys. Rev. A **51**, 2112 (1995).
[20] M. A. Kornberg and J. E. Miraglia, Phys. Rev. A **49**, 5120 (1994).
[21] A. I. Mikhailov, I. A. Mikhailov, A. N. Moskalev, A. V. Nefiodov, G. Plunien, and G. Soff, Phys. Rev. A **69**, 032703 (2004).

[22] A. I. Mikhailov, A. V. Nefiodov, and G. Plunien, J. Phys. B: At. Mol. Opt. Phys. **42**, 231003 (2009).

[23] J. Hoszowska, A. K. Kheifets, J.-Cl. Dousse, M. Berset, I. Bray, W. Cao, K. Fennane, Y. Kayser, M. Kavčič, J. Szlachetko, and M. Szlachetko, Phys. Rev. lett. **102**, 073006 (2009).

[24] A. S. Kheifets, I. Bray, and J. Hoszowska, Phys. Rev. A **79**, 042504 (2009).

[25] R. Wehlitz and S. B. Whitfield, J. Phys. B: At. Mol. Opt. Phys. **34**, L719 (2001).

[26] J. B. Bluett, D. Lukic, S. B. Whitfield, and R. Wehlitz, Nucl. Instrum. Methods B **241**, 114 (2005).